

See discussions, stats, and author profiles for this publication at: <https://www.researchgate.net/publication/224541489>

# Efficient generation and sorting of orbital angular momentum eigenmodes of light by thermally tuned q-plates

Article in *Applied Physics Letters* · July 2009

DOI: 10.1063/1.3154549 · Source: IEEE Xplore

CITATIONS

287

READS

381

5 authors, including:



**Ebrahim Karimi**

University of Ottawa

332 PUBLICATIONS 13,287 CITATIONS

[SEE PROFILE](#)



**Bruno Piccirillo**

University of Naples Federico II

105 PUBLICATIONS 5,191 CITATIONS

[SEE PROFILE](#)



**Enrico Santamato**

University of Naples Federico II

153 PUBLICATIONS 6,757 CITATIONS

[SEE PROFILE](#)

# Efficient generation and sorting of orbital angular momentum eigenmodes of light by thermally tuned q-plates

Ebrahim Karimi,<sup>1,2</sup> Bruno Piccirillo,<sup>1,3</sup> Eleonora Nagali,<sup>4</sup> Lorenzo Marrucci,<sup>1,2</sup> and Enrico Santamato<sup>1,3</sup>

<sup>1</sup>*Dipartimento di Scienze Fisiche, Università di Napoli “Federico II”,  
Compl. Univ. di Monte S. Angelo, 80126 Napoli, Italy*

<sup>2</sup>*Consiglio Nazionale delle Ricerche-INFM Coherentia, Napoli, Italy*

<sup>3</sup>*Consorzio Nazionale Interuniversitario per le Scienze Fisiche della Materia, Napoli*

<sup>4</sup>*Dipartimento di Fisica, Università di Roma “La Sapienza”, 00185 Roma, Italy*

We present methods for generating and for sorting specific orbital angular momentum (OAM) eigenmodes of a light beam with high efficiency, using a liquid crystal birefringent plate with unit topological charge, known as “q-plate”. The generation efficiency has been optimized by tuning the optical retardation of the q-plate with temperature. The measured OAM  $m = \pm 2$  eigenmodes generation efficiency from an input TEM<sub>00</sub> beam was of 97%. Mode sorting of the two input OAM  $m = \pm 2$  eigenmodes was achieved with an efficiency of 81% and an extinction-ratio (or cross-talk) larger than 4.5:1.

A light beam has two “rotational” degrees of freedom: spin angular momentum (SAM) and orbital angular momentum (OAM). Light SAM is related to the vectorial properties of the transverse electric field and may take two values  $s = +1$  and  $s = -1$  (in units of  $\hbar$ ), corresponding to left and right circularly polarized light, respectively. Light OAM is defined by the phase structure of the complex electric field [1] and may take any of the infinite values  $m = 0, \pm 1, \pm 2, \dots$ . In the last decade, the interest in light beams endowed with OAM has continuously increased, because of the wide range of scientific and technological applications in both classic [2] and quantum regimes of light [3, 4]. Till today, only few tools have been developed for generating and manipulating OAM, including pitch-fork holograms [5], spiral phase plates [6, 7], Dove prisms, Leach’s interferometers [8], and cylindrical lens mode converters [9]. All these devices and techniques have drawbacks and limitations in terms of efficiency, modulation speed, working wavelength, alignment, and constraints imposed on the input and output beams.

Recently, a novel optical device for the OAM manipulation has been introduced, made as a birefringent liquid crystal plate having a azimuthal distribution of the local optical axis in the transverse plane, with a topological charge  $q$  at its center defect, hence named “q-plate” (QP). When a light beam traverses a QP, the topological charge  $2q$  is transferred into the phase of the beam, which thus gains a corresponding amount of OAM, with a sign determined by the light input polarization. In this paper we consider only QP with  $q = 1$ , having cylindrical symmetry around their central defect. Because of this symmetry, a  $q = 1$  QP cannot change the total SAM + OAM angular momentum of the incident beam, so that its action is just that of converting the SAM-variation of some photons into OAM, and *vice versa* (SAM-to-OAM-conversion, or STOC) [10]. Besides the topological charge  $q$ , the QP is characterized by its birefringent retardation  $\delta$ , ideally uniform in the trans-

verse plane, which determines the STOC efficiency, i.e. the fraction of photons (or optical energy) that is actually converted. Moreover, QPs are highly transparent and can be cascaded along the beam to produce arbitrary values (even, if  $q = 1$ ) of the OAM [11]. The STOC efficiency can ideally touch 100% [12]. In this work we achieved STOC efficiencies exceeding 95%, to be compared, for example, with the record efficiencies ranging from 50% to 90%, depending on the wavelength, of computer-generated blazed fork holograms [13, 14]. High efficiencies in producing and detecting the light OAM are highly desirable in all circumstances where only few photons are at disposal. Examples are weak signals coming from far sources, such as astronomical ones, [15] or after propagation in highly absorbing media, or in quantum information applications. Achieving high efficiencies, however, requires accurate tuning of the QP retardation  $\delta$ . In order to tune the optical retardation  $\delta$  and thus optimize the QP efficiency, in this work we adopted a method based on controlling the material temperature, which presents good features in terms of a realization simplicity and stability of the obtained retardation.

This paper is divided in two parts, the first dealing with OAM generation and the second with OAM sorting, e.g., for detection purposes. In the first experiment, we used the STOC process for transforming an input TEM<sub>00</sub> laser beam into a beam having OAM  $m = \pm 2$ . Our QP was manufactured as a  $6\mu\text{m}$  thick film of E7 liquid crystal from Merck, sandwiched between two circularly rubbed glass substrates coated with the polyimide PI2555 from DuPont. The transmittance  $T$  of our QP was measured to be 88%, with the losses arising from scattering due to manufacturing imperfections and from the lack of antireflection coating on the cell bounding glasses. The optical setup used to measure the STOC efficiency of our QP as a function of its optical retardation is shown in Fig. 1. The input light was a linearly polarized TEM<sub>00</sub> laser beam generated by a frequency-doubled continuous-wave Nd:YVO<sub>4</sub> ( $\lambda = 532\text{ nm}$ ). After changing the polariza-

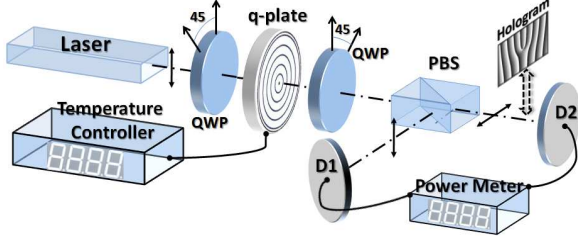


FIG. 1: Setup to measure the STOC efficiency and the state purity. Legend: QWP - quarter-wave plate; PBS - polarizing beam-splitter. The fork hologram was inserted on the converted beam arm for verifying the degree of purity of the OAM  $m = 2$  mode generated on the output.

tion into left-circular ( $L$ ) by a suitably oriented quarter wave plate (QWP), the beam was made to pass through our controlled-temperature QP. In the QP, a fraction of the photons will undergo the STOC process and will therefore emerge with right-circular ( $R$ ) polarization and OAM  $m = 2$ , and the others will remain in the OAM  $m = 0$  and with  $L$  polarization. For arbitrary QP tuning, the transverse intensity pattern of the beam emerging from the QP exhibits a central spot, corresponding to the light fraction that is left in the initial OAM state  $m = 0$ , surrounded by a single ring, corresponding to the light converted into the OAM  $m = 2$  mode (doughnut beam). By inserting in the output beam a second QWP and a polarizing beam-splitter (PBS) oriented so as to select the  $R$ -polarization for, say, the transmission output, a pure doughnut beam is obtained. The reflected output of the PBS shows instead only the central spot (unconverted light). If  $P_{in}$  is the total input power, the respective powers of the coherently converted and unconverted components,  $P_{R,2}$  and  $P_{L,0}$ , are expected to depend on the optical retardation  $\delta$  according to the following Malus-like laws [12, 16]:

$$P_{R,2} = P_0 \sin^2 \frac{\delta}{2} \quad P_{L,0} = P_0 \cos^2 \frac{\delta}{2} \quad (1)$$

where  $P_0 = TP_{in}$  is the total power transmitted coherently by the QP. To adjust the retardation  $\delta$ , the temperature of the QP was varied while measuring the power of the two output beams of the PBS. The results are shown in Fig. (2), together with best-fit curves based on Eqs. (1), assuming a second-order polynomial dependence  $\delta(T) = a + bT + cT^2$  and adding a constant offset of 0.5% that accounts for the finite PBS and waveplates contrast ratios. When the PBS-transmitted power (full squares in Fig. (2)) reaches its maximum, we obtain the optimal STOC and almost all photons emerge in the  $m = 2$  OAM state. More precisely, in this optimal situation, about 99.2% of the beam power is transmitted by the PBS, and after taking into account the finite contrast ratio of the waveplates and PBS (as measured without the QP), the actual QP efficiency in inverting the optical

polarization is estimated to be 99.6%. Near the minima of the same curve, the STOC process is minimum and almost all photons emerge in the original  $m = 0$  state.

To test the purity of the OAM eigenmode generated by

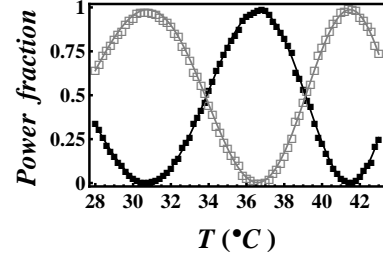


FIG. 2: STOC power fraction  $P_{R,2}/P_0$  (black squares) and no STOC power fraction  $P_{L,0}/P_0$  (empty squares) as functions of the QP temperature. The curve is the best fit obtained as explained in the text.

our QP, at the optimal temperature we inserted along the beam a double pitchfork hologram as OAM-mode splitter [5, 13] and, on the first-order diffracted beam we selected the central spot by a suitable iris placed before the detector. After suitable calibration of the detection efficiency, the measured OAM  $m = 2$  mode content fraction was estimated to be  $F = 97.2\%$  (in quantum optics,  $F$  is the squared “fidelity” to the desired mode  $m = 2$ ), so that the overall QP efficiency in generating a pure OAM  $m = 2$  mode is  $\eta = 97.2\% \times 99.6\% = 96.9\%$  (this value is net of reflection and scattering losses in the QP; including all losses, the efficiency of our QP is 85%, a figure which could be however easily improved to more than 90% by simply adding antireflection coatings). Moreover, we note that in order to invert the sign of the generated OAM value  $m$  (e.g., from  $+2$  to  $-2$ ) with our setup it is enough to switch the input and output polarizations to the orthogonal ones. This can be achieved at gigaHertz rates by means of Pockel cells. No switching capability is instead possible with passive holograms, while computer-controlled spatial light modulators (SLM) can achieve at most switching rates of the order of few kiloHertz.

Let us now discuss the second experiment, about OAM mode sorting. More precisely, we present a setup for sorting the four modes given by combining the two OAM modes  $m = 2$  and  $m = -2$  and the two orthogonal polarizations  $L$  and  $R$ . The setup is similar to the previous one, except that the input laser beam was made to pass through a SLM driven with a computer generated hologram (CGH) for determining its input OAM state. The temperature of the QP was held fixed at the optimal value for maximum STOC efficiency. We used double-pitchfork CGHs to produce alternatively  $m = 2$  and  $m = -2$  OAM eigenstates in the input. The first QWP was also rotated so as to produce, alternatively, right-circular and left-circular polarizations. In this way, we created in sequence the four photon states  $|L, 2\rangle$ ,  $|L, -2\rangle$ ,

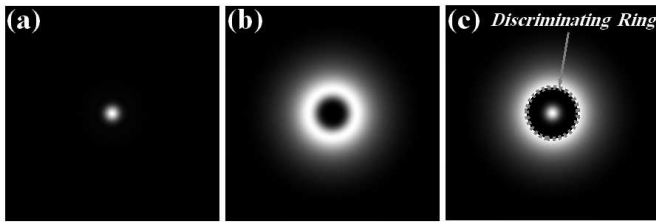


FIG. 3: Calculated far-field patterns of OAM modes  $m = 0$  and  $m = 4$ , generated by the q-plate for input OAM  $m = \pm 2$  (The input beam was assumed  $\text{HyGG}_{-2,\pm 2}(r, \phi, 0.1)$  [17] mode). The dashed circle shows the discriminating area used in the balanced mode sorter.

$|R, 2\rangle, |R, -2\rangle$ , where the first symbol in the ket denotes the polarization and the second is the  $m$  value of the photon OAM. Because the STOC process is complete in a tuned QP, after passing through the QP these four states are expected to change respectively into  $|R, 4\rangle, |R, 0\rangle, |L, 0\rangle, |L, -4\rangle$ . The QWP after the QP, changes these states into  $|H, 4\rangle, |H, 0\rangle, |V, 0\rangle, |V, -4\rangle$ , respectively, so that the two states  $|H, 4\rangle, |H, 0\rangle$  are transmitted by the PBS and the other two states  $|V, 0\rangle, |V, -4\rangle$  are reflected. We see that owing to the QP, the two states in each of the reflected and transmitted beam have a different value of photon OAM ( $m = 0$  and  $m = 4$ ). After propagating in the far-field (or in the focal plane of a lens), these two modes can then be separated by exploiting their different radial distribution, i.e., a central spot for  $m = 0$  and an outer ring for  $m = 4$ , as shown in Fig. (3), thus finally sorting all four initial spin-orbit modes into separate beams. The radial sorting can be obtained, for example, by means of a mirror with a hole at its center. We note that in our measurements we are using the PBS only for discriminating the two input polarizations. In many applications, the input polarization state is fixed and known and one is interested only in sorting the OAM  $m = \pm 2$  modes. In this case, the PBS is unnecessary, the input light can be always made  $L$ -polarized, by suitable wave plates, and the output beam will then be only  $R$ -polarized. The OAM sorting is then still based on the radial-mode separation in the far field. The efficiency of this mode-sorter, here defined as the fraction of the optical power in a given eigenmode to be sorted that is directed in the *correct* output mode is however not 100%, because of the radial mode overlap, leading to some energy going in the “wrong” OAM output mode. This also leads also to a finite contrast ratio, i.e., to cross-talk between the input channels. In Table I we report the measured efficiencies and contrast ratios for the four input spin-orbit base states previously mentioned, with a discriminating hole radius chosen so as to balance the output efficiencies for opposite input OAM (see Fig. (3)). The measured efficiency of the QP as mode sorter is of about 81.5% (72% with QP losses),

i.e., 2.7 times larger than for the best available holograms ( $\approx 30\%$  efficiency, as blazing cannot be used for multiple outputs). The extinction ratio due to radial overlap between  $m = 0$  and  $m = 4$  OAM modes can be improved by introducing a suitable opaque belt mask that cuts away the overlapping region of the two modes, although at the expense of a reduced efficiency. In principle the contrast ratio can be made arbitrarily large. Theoretically, we estimate a contrast ratio  $> 10^3$  for an efficiency of about 50% and  $> 10^6$  for an efficiency of 10%. We note that the radial-overlap problem leading to cross-talk is not unique of the QP approach; a similar problem and an equivalent efficiency/contrast-ratio tradeoff is present also with hologram-based OAM sorting. We also tested our QP mode-sorter with coherent superpositions of  $m = +2$  and  $m = -2$  OAM modes (obtained with suitable CGHs), obtaining results consistent with the efficiencies reported in Table I.

In conclusion, we demonstrated the application of a liq-

TABLE I: The QP’s efficiency as a mode sorter.

Input state	Output state	Efficiency	Extinction ratio
$ L, 2\rangle$	$ R, 4\rangle$	81.1%	$\approx 4.6:1$
$ L, -2\rangle$	$ R, 0\rangle$	81.8%	$\approx 4.5:1$
$ R, 2\rangle$	$ L, 0\rangle$	81.6%	$\approx 4.7:1$
$ R, -2\rangle$	$ L, -4\rangle$	81.5%	$\approx 4.6:1$

uid crystal q-plate as (i) a switchable OAM generator and (ii) a OAM mode-sorter, exploiting the optical spin-to-orbital angular momentum conversion process. By suitable thermal tuning of the birefringent retardation in the q-plate, we optimized its generation or mode-sorting efficiency, finding values as large as  $\approx 97\%$  as mode generator and  $\approx 81\%$  as mode sorter. These results show that the q-plates can easily reach much larger efficiencies than holographic elements and will therefore provide the most convenient option for many applications, particularly when low photon fluxes are available.

- 
- [1] L. Allen, S. M. Barnett, and M. J. Padgett, *Optical angular momentum*, Institute of Physics Publishing, Bristol, (2003).
  - [2] G. Gibson, J. Courtial, M. J. Padgett, M. Vasnetsov, V. Pasko, S. M. Barnett, and S. Franke-Arnold, *Opt. Express* **12**, 5448 (2004).
  - [3] A. Mair, A. Vaziri, G. Welhs, and A. Zeilinger, *Nature* **412**, 313 (2001).
  - [4] G. Molina-Terriza, J. P. Torres, and L. Torner, *Nat. Phys.* **3**, 305 (2007).
  - [5] V. Y. Bazhenov, M. V. Vasnetsov, and M. S. Soskin, *JETP Lett.* **52**, 429 (1990), [*Pis’ma Zh. Eksp. Teor. Fiz.* **52**, 1037(1990)].
  - [6] M. W. Beijersbergen, R. P. C. Coerwinkel, M. Kristensen, and J. P. Woerdman, *Opt. Commun.* **112**, 321

- (1994).
- [7] K. Sueda, G. Miyaji, N. Miyanaga, and M. Nakatsuka, *Opt. Express*. **12**, 3548 (2004).
  - [8] J. Leach, J. Courtial, K. Skeldon, S. M. Barnett, S. F. Arnold, and M. J. Padgett *Phys. Rev. Lett.* **92**, 013601 (2004).
  - [9] L. Allen, M. W. Beijersbergen, R. J. C. Spreeuw, and J. P. Woerdman, *Phys. Rev. A* **45**, 8185 (1992).
  - [10] L. Marrucci, C. Manzo, and D. Paparo, *Phys. Rev. Lett.* **96**, 163905 (2006).
  - [11] L. Marrucci, C. Manzo, and D. Paparo, *Appl. Phys. Lett.* **88**, 221102 (2006).
  - [12] E. Karimi, B. Piccirillo, L. Marrucci, and E. Santamato, *Opt. Lett.* **34**, 1225 (2009).
  - [13] N. R. Heckenberg, R. McDuff, C. P. Smith, H. Rubinsztein-Dunlop, and M. J. Wegener, *Opt. Quantum Electron.* **24**, S951 (1992).
  - [14] H. He, N. R. Heckenberg, and H. Rubinsztein-Dunlop, *J. Mod. Opt.* **42**, 217 (1995).
  - [15] M. Harwit, *Astrophys. J.* **597**, 1266 (2003).
  - [16] L. Marrucci, *Mol. Cryst. Liq. Cryst.* **488**, 148 (2008).
  - [17] E. Karimi, G. Zito, B. Piccirillo, L. Marrucci, and E. Santamato, *Opt. Lett.* **32**, 3053 (2007).